PHYSICAL REVIEW D

PARTICLES AND FIELDS

THIRD SERIES, VOLUME 38, NUMBER 7 1 OCTOBER 1988

Antiproton-proton annihilation at rest into $\pi^0 M$ and γM with $M=\phi, \eta', \omega, \rho^0, \eta$, and π^0

M. Chiba,[e] T. Fujitani,[d] J. Iwahori,[a,*] M. Kawaguti,[a] M. Kobayashi,[b] S. Kurokawa,[b] Y. Nagashima,[d] T. Omori,[d,†] S. Sugimoto,[d] M. Takasaki,[b] F. Takeutchi,[c] Y. Yamaguchi,[d] and H. Yoshida[a]

[a]*Faculty of Engineering, Fukui University, Fukui 910, Japan*

[b]*National Laboratory for High Energy Physics (KEK), Tsukuba, Ibaraki 305, Japan*

[c]*Faculty of Science, Kyoto Sangyo University, Kita, Kyoto 603, Japan*

[d]*Physics Department, Osaka University, Toyonaka, Osaka 560, Japan*

[e]*Physics Department, Tokyo Metropolitan University, Setagaya, Tokyo 152, Japan*

(Fukui–KEK–Kyoto Sangyo–Osaka–Tokyo Metropolitan Collaboration)

(Received 29 January 1988)

We have carried out high-statistics measurements of inclusive π^0 and γ-ray spectra from $\bar{p}p$ annihilation at rest. From the monochromatic peaks in the π^0 spectra, we derive the yield (or its upper limit) of the reaction $\bar{p}p \to \pi^0 M$ for $M=\phi, \eta', \omega, \rho^0, \eta$, and π^0. The same quantity was independently obtained from the γ-ray spectra, which included some π^0's that were mistaken as single γ rays due to the limited granularity of the γ detector. Taking the monochromatic peaks in the γ-ray spectra as being due to prompt γ rays, we also derive the upper limit for $\bar{p}p \to \gamma M$.

I. INTRODUCTION

Much interest has been paid to $\bar{p}p$ annihilation at rest which produces a π^0 plus a neutral meson M. One of the interesting aspects of this reaction is the ratio of annihilation from P states (generally odd-L states) to that from S states (even-L states).[1–4] The predominance of an S wave has been assumed, since the absorption in π^-, K^-, and Σ^- atoms is known[5] to occur predominantly from S states. The ratio of P-wave annihilation can be obtained from $\bar{p}p \to \pi^0\pi^0$, which cannot occur from S states because of parity and C-parity invariance. Assuming a charge independence between the above reaction and $\bar{p}p \to \pi^+\pi^-$, which can occur from both P and S states, we can write the ratio R of P-wave annihilation to all annihilation in $\bar{p}p \to \pi\pi$ as

$$R = 3B(\bar{p}p \to \pi^0\pi^0)/[B(\bar{p}p \to \pi^+\pi^-) + B(\bar{p}p \to \pi^0\pi^0)] , \quad (1)$$

where B denotes the yield per annihilation (branching ratio). Previous experimental values[1–3] of R varied between 0.13 and 0.39. Since $B(\bar{p}p \to \pi^+\pi^-)$ is known rather precisely, a precise measurement of $B(\bar{p}p \to \pi^0\pi^0)$ is important in determining R. Measurements of $\bar{p}p \to \pi^0\eta$ and $\pi^0\eta'$ are also interesting since these reactions are again inhibited in the S-wave annihilation because of parity and C-parity invariance.

Another interesting subject is quark and gluon dynamics, which can be studied in terms of the branching ratios into various two-meson channels. In particular, annihilation at rest into two neutral mesons belonging to the light pseudoscalar (PS) nonet is one of the best research grounds[5,6] for the above subject, since all the channels are energetically accessible. Using a quark-line-rule (QLR) approach,[7] Genz[6] has argued in favor of the dominance of annihilation graphs [without quark-line crossing, see Fig. 1(a)] over rearrangement ones [with quark-line crossing, see Fig. 1(b)]. The relative yields among $\bar{p}p \to \pi^0\pi^0$, $\pi^0\eta$, $\pi^0\eta'$, $\eta\eta$, $\eta\eta'$, $\eta'\eta'$, etc., also allow for an independent determination[6] of the PS mixing angle θ_{PS}, which has been determined from the mass formula. Dover and Fishbane,[8] analyzing $\bar{p}p$ annihilation at rest

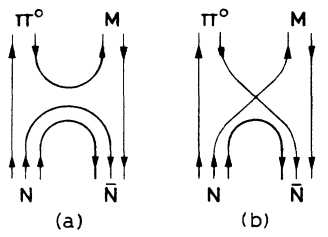

FIG. 1. Quark graphs for $\bar{p}p$ annihilation into two mesons: (a) quark annihilation (planar) and (b) quark rearrangement graphs.

into two PS mesons (for example, $\bar{p}p \to K^+K^-$), showed that both annihilation and rearrangement graphs are important. They pointed out that annihilation into two PS mesons reveals interference effects between both graphs. An interesting example is the ratio $R' = B(\bar{p}p \to \pi^0\eta)/B(\bar{p}p \to \pi^0\pi^0)$. Rearrangement graphs predict R' to be much smaller than unity, while annihilation graphs predict values as large as unity. The available experimental values of R' differ by almost a factor of 40 between 0.4 and 15. A precise determination of R' would indicate which process should dominate. Hartmann *et al.*,[9] following a slightly different approach [use of SU(3)-invariant amplitudes] and using experimental data of $\bar{p}p$ annihilation into two PS mesons (K^+K^-, K^0K^0, $\pi^+\pi^-$), also showed that both annihilation and rearrangement graphs are important. They also showed the predominance of rearrangement graphs in the C-parity-even $\bar{p}p$ annihilation into a PS meson plus a vector one.

Experimental data concerning $\bar{p}p \to \pi^0 M$ are scarce, especially when the decay of M involves π^0. This is because most experiments have been carried out with bubble chambers and because π^0 measurements in counter experiments usually require precision γ detectors of large acceptance, which are not easily constructed. This paper reports an experimental result[10] concerning $\bar{p}p$ annihilation at rest into $\pi^0 M$ for $M = \phi$, η', ω, ρ^0, η, and π^0. The yield was primarily derived from monoenergetic peaks in the inclusive π^0 spectra, which were measured separately for various charge multiplicities. It was also independently obtained, though with poorer statistics, from monoenergetic peaks in the inclusive γ-ray spectra. This was possible since some π^0 mesons were apparently registered as single γ rays because of an incomplete separation of two γ rays from π^0 due to the finite granularity of the γ detector. The monoenergetic peaks in the γ-ray spectra may partially originate from prompt γ rays produced in the radiative annihilation of $\bar{p}p \to \gamma M$. Attributing the peaks entirely to $\bar{p}p \to \gamma M$, we also deduced the upper limit for $\bar{p}p \to \gamma M$.

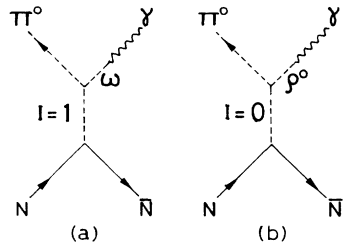

FIG. 2. Quark graphs with a single intermediate meson state in the s channel for an example of radiative annihilation $\bar{p}p \to \gamma\pi^0$: (a) isospin $I = 1$ and (b) $I = 0$ amplitudes.

Before concluding this Introduction we briefly comment on $\bar{p}p \to \gamma M$, one of the by-products measured in the present experiment. $\bar{p}p \to \gamma M$ can be simply treated[11] in a model using a single intermediate meson state in the s channel (see Fig. 2) and can give information concerning the interference between two amplitudes with isospins $I = 0$ and 1. As an example, $\bar{p}p \to \gamma\pi^0$ should predominantly proceed from the initial $^1S_0$ state; its yield is given by[11]

$$B(\bar{p}p \to \gamma\pi^0) = \{B(\bar{p}p \to \pi^0\omega)/9 + \tfrac{2}{3}\cos\beta' \sqrt{B(\bar{p}p \to \pi^0\omega)B(\bar{p}p \to \pi^0\rho^0)} + B(\bar{p}p \to \pi^0\rho^0)\} A^2 C \ , \quad (2)$$

where $A = eg_{\rho\gamma}/m_\rho^2 = 0.055$, and $C = k(\pi^0\gamma)/k(\pi^0\rho^0)$ with $k(\pi^0\gamma)$ and $k(\pi^0\rho^0)$ the final-state momenta in the reaction $\bar{p}p \to \pi^0\gamma$ and $\bar{p}p \to \pi^0\rho^0$, respectively. If $B(\bar{p}p \to \pi^0\gamma)$, $B(\bar{p}p \to \pi^0\omega)$, and $B(\bar{p}p \to \pi^0\rho^0)$ are experimentally obtained, Eq. (2) gives the phase of the interference, β'.

II. EXPERIMENT

The experimental setup was described in Ref. 12. Antiprotons at 580 MeV/c were selected according to their time of flight in the K4 beam line of the KEK 12-GeV proton synchrotron, degraded in a graphite degrader, tracked in multiwire proportional chambers (MWPC's), and finally stopped in a 3.3-liter liquid-hydrogen target. Secondary charged particles were detected with scintillator hodoscopes and tracked with cylindrical as well as planar MWPC's, with a total coverage of about 93% of 4π sr. The actual tracking efficiency for each charged particle was about 90%. The annihilation vertex was determined from the tracks of the primary and the secondary charged particles. If the final state had no charged particles, the vertex was determined from dE/dx of the projectile slow antiprotons (measured with a Si solid-state detector).

γ rays were measured with a calorimeter[13] comprising 96 NaI(Tl) and surrounding 48 scintillating glass modules assembled in a half-barrel configuration around the beam axis. The hydrogen target was located at the center of the barrel. The useful acceptance of the NaI for γ rays was about 22%; the leaking energies were measured in the scintillating glass. The geometrical acceptance for π^0, for the sum of separated and unseparated 2γ rays, increased with the π^0 total energy: 10.5% at 500 and 14.5% at 900 MeV.

The effective energy resolution of the NaI detector for γ rays [full width at half maximum (FWHM)] was[12]

$$\Delta E_\gamma/E_\gamma = 0.062/(E_\gamma \text{ in GeV})^{1/4} \ . \quad (3)$$

The overall energy resolution for π^0 could also be approximated using the same formula as above, with E_γ replaced by the π^0 energy E. The gain of the γ modules was monitored to within 1% throughout the experiment and corrected for in the software analysis. The energy scale was calibrated to within 2% using the 129-MeV γ rays (Panofsky γ rays) and the 780-MeV π^0 from $\bar{p}p \to \pi^0\rho^0/\omega$ (sum of $\pi^0\rho^0$ and $\pi^0\omega$).

III. DATA REDUCTION

Events which had one or two γ rays in the NaI were triggered irrespective of the multiplicity of the charged particles. The present data were collected while using the same sample mentioned in Ref. 12, in which a search for monochromatic γ rays accompanying baryonium production was carried out. The data reduction for π^0's was similar to that for γ rays[12] except for a minor difference in the vertex cut. From 3.6×10^7 triggered events, we removed spurious incident-beam events as well as events for which tracking of the antiprotons downstream of the degrader failed. Vertex reconstruction, carried out for the 2.7×10^7 accepted events, was successful for 1.75×10^7 events after the following cuts: (i) the rms distance from the vertex to the charged tracks should be less than 3 cm and (ii) the vertex should not be located outside the target cell by more than 1.5 cm either radially or longitudinally.

γ rays were identified by energy deposits in the NaI and by the absence of signals in the scintillator hodoscope as well as in the MWPC in front of the hit NaI modules. Each cluster of energy deposits, i.e., a γ ray, was isolated from neighboring clusters by using a cluster-finding logic in the software analysis. "Hit" or "not hit" was first assigned to each module with a discriminating threshold of 0.7 MeV. The hit modules were grouped into connected regions. Peaks of energy deposits were then picked up in each connected region. A region with only one peak was taken as a cluster. A region with two peaks was taken as two clusters only when the peaks were separated by at least one module with an energy less than the peaks by more than 5%. When a connected region was divided into two clusters, some modules should have been shared between them. Instead of sharing, such modules were simply connected to one of the neighboring modules with the highest energy deposit. After having thus selected γ rays, we required for each γ ray that the energy leakage from the NaI to the scintillating glass should be less than 10%, and finally obtained $N_\gamma=1.60\times10^7$ γ rays above 10 MeV.

Although most of the π^0's were detected as two separate γ rays, some percentage of the π^0's were mistaken as single γ rays. Consequently, π^0 from $\bar{p}p\to\pi^0 M$ could create a monoenergetic peak both in the inclusive π^0 and in the inclusive γ-ray spectra. For the mesons M of interest, the π^0 energy ranged from 666 MeV (for $M=\phi$) to 938 MeV ($M=\pi^0$). The minimum opening angle between two decay γ rays ranged from 23.4° at 666 MeV to 16.5° at 938 MeV. Although an angle of 10° subtended by each γ module at the target was smaller than the above-mentioned values, the separation between two γ rays became incomplete with increasing π^0 energy because of finite size of the shower. The occurrence of a monoenergetic peak in the γ-ray spectra is sketched in Fig. 3 for the reaction $\bar{p}p\to\pi^0\omega$. γ rays from a 780-MeV π^0 have a box-shape energy distribution between 5.9 and 774.1 MeV. According to a Monte Carlo calculation, about 20% of the π^0's falling on the γ detector were registered as single γ rays at the same energy as the π^0's (see the shaded peak in Fig. 3). Then $\bar{p}p\to\pi^0\omega$ should show up in the inclusive γ-ray spectra as a broad background

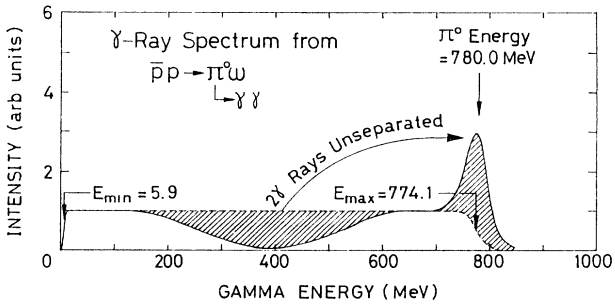

FIG. 3. A schematic sketch for the occurrence of a monochromatic π^0 meson peak in the inclusive γ-ray spectra for an example of $\bar{p}p\to\pi^0\omega$. The energy distribution of the decay γ rays is of a box shape from $E_{\min}$ to $E_{\max}$. The γ-ray energies are around 390 MeV when the $\gamma\gamma$ opening angle is close to the minimum. Such 2γ rays are partially unseparated and registered as a single γ ray owing to the finite granularity of the γ detector (see the text).

plus a monoenergetic peak at 780 MeV, whose width is determined by the instrumental resolution.

The acceptances for detecting π^0 as two separate γ rays and an unseparated single γ ray, $\alpha(2\gamma)$ and $\alpha(1\gamma)$, respectively, were calculated[12] by a Monte Carlo simulation, in which γ-ray showers were simulated by the EGS program.[14] We first calculated the energy dependence of $\alpha(1\gamma)$ by neglecting the γ-detector walls, which should make the shower calculation complicated. We then renormalized the result at 785 MeV so that the experimental yields of the prominent $\bar{p}p\to\pi^0\rho^0/\omega$ channel (sum of $\pi^0\rho^0$ and $\pi^0\omega$) obtained from the inclusive π^0 and the inclusive γ-ray spectra should agree with each other. The calculated $\alpha(2\gamma)$ and $\alpha(1\gamma)$ are plotted in Fig. 4. The dashed curves give the acceptances for isolated π^0, while the solid curves give those for π^0 coming from $\bar{p}p$ annihilation at rest. The latter is smaller due to the trigger condition and to a loss of the π^0's that overlap other annihi-

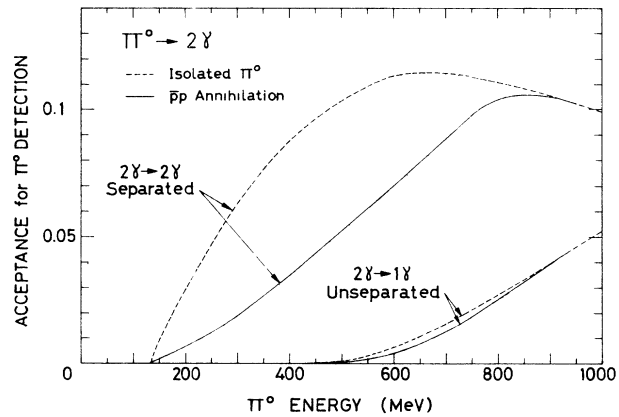

FIG. 4. Acceptances $\alpha(2\gamma)$ and $\alpha(1\gamma)$ of the NaI(Tl) detector (Ref. 13) for detecting $\pi^0\to2\gamma$ separately and mistaking them for a single γ, respectively (see the text for separation criteria). Dashed and solid curves give the acceptances for isolated π^0 and π^0 produced in $\bar{p}p$ annihilation, respectively.

lation products. $\alpha(1\gamma)$ was less than 1% below 600 MeV, increasing with energy up to 3.9% at 900 MeV.

For events in which more than one γ ray hit the NaI, the $\gamma\gamma$ invariant mass, denoted as $M(\gamma\gamma)$, was calculated for all possible combinations. The photon vector was taken from the vertex to the center of gravity of the shower. When the cylinder coordinate system (r,ϕ,z) was referred to with the z axis along the beam axis, (ϕ,z) of the center of gravity were obtained from the energy distribution among the γ modules. The r coordinate was determined so that the depth of the vertex in the NaI along the photon vector was, according to Rossi's approximation-B formula,[15] $1.01\times\ln(\gamma$ energy/critical energy$)+1.2$ in units of radiation lengths. The $M(\gamma\gamma)$ spectra are presented in Fig. 5 for the sum over the charge multiplicity, $N_{\rm ch}$, and elsewhere[16] separately for each $N_{\rm ch}$. The π^0 peak was observed at 134 MeV with an rms width of 13.0 MeV. The π^0 mass resolution is related to those of two γ energies, k_1 and k_2, and of the opening angle θ between the two γ rays in the following way:

$$\frac{\sigma(M(\gamma\gamma))}{M(\gamma\gamma)}=\frac{1}{2}\left[\left[\frac{\sigma(k_1)}{k_1}\right]^2+\left[\frac{\sigma(k_2)}{k_2}\right]^2+\left[\frac{\sin\theta\sigma(\theta)}{1-\cos\theta}\right]^2\right]^{1/2}, \tag{4}$$

where the rms errors, $\sigma(k_1)$ and $\sigma(k_2)$, are given by Eq. (3). The rms angular error $\sigma(\theta)$ was estimated from the Monte Carlo procedure to be 2 to 5 degrees, depending on the injection angle of γ rays to the NaI. The π^0 mass resolution was dominated by the angular error term and was consistent with the obtained value of 13.0 MeV. We selected π^0 by a $\pm2.0\sigma$ mass cut (indicated by arrows in Fig. 5). The number of true π^0 above the background was $N_\pi=1.36\times10^6$ with a true-to-background ratio of 7/3. The π^0 energy spectra are presented in Fig. 6. One-, three-, and five-pronged events, which occurred due to small inefficiency in tracking and to $\gamma\rightarrow e^+e^-$ conversion, were included in the spectra of two-, four-, and six-pronged events, respectively.

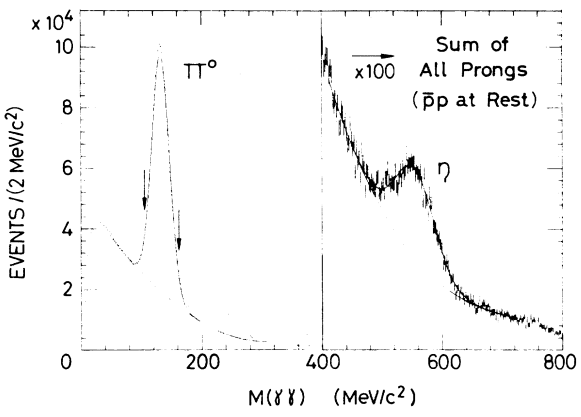

FIG. 5. The $\gamma\gamma$ invariant-mass spectrum summed over $N_{\rm ch}$. The solid curve gives a fit of the π^0 peak with a polynomial plus a Gaussian shape. The η peak is also shown.

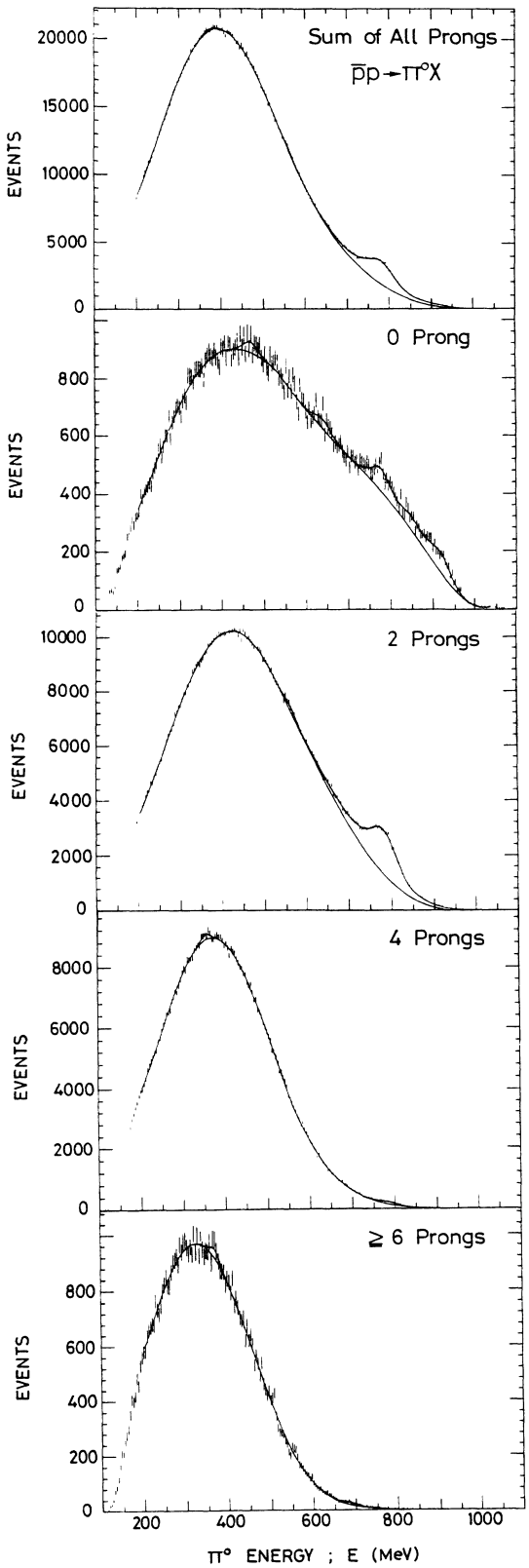

FIG. 6. The inclusive π^0 spectra for each charge multiplicity as well as for their sum. The solid curves show fits with a polynomial background plus narrow peaks (see the text). They are drawn after connecting the fits over various energy windows smoothly at the energies where no peaks were seen. The bin width is 4.16 MeV.

IV. RESULT ON $\bar{p}p \to \pi^0 M$ FROM π^0 SPECTRA

We searched for monoenergetic peaks in the inclusive π^0 spectra at energies corresponding to $\bar{p}p \to \pi^0 M$ with $M = \phi$, η', ω, ρ^0, η, and π^0. The π^0 energy varied from 666 MeV for $M = \phi$ to 938 MeV for $M = \pi^0$. We did not consider higher-mass mesons such as $f(1270)$, $A_1(1270)$, $D(1285)$, $A_2(1320)$, etc., because they are broad, and/or overlap each other, and/or sit close to the crest of the π^0 spectra. A search was made by fitting the π^0 spectra with a polynomial background plus narrow peaks by employing the minimization program MINUIT.[17] The peaks were approximated by Gaussian curves except for ρ^0, which should have a Breit-Wigner shape. The peak position was variable while the Gaussian width was bound within the instrumental width $\pm 20\%$. To reduce the number of adjustable parameters, the fitting was made in a few to several π^0 energy windows having ranges up to 400 MeV. The fitted result is shown in Fig. 6 with solid curves and is also summarized in Table I. The quoted error (1σ) for the peak area is the larger one of the MINUIT error and the statistical error of the background lying under the peak within $\pm$instrumental FWHM. The residue after subtracting the background is shown in Fig. 7. $\bar{p}p \to \pi^0\rho^0/\omega$, $\pi^0\eta$, and $\pi^0\pi^0$ gave significant peaks (more than 10σ, 3σ, and 7σ effects, respectively), while the other channels gave peaks at only 1 to 2σ levels. The 2σ peak seen at a π^0 energy of 562 MeV does not correspond to any known mesons with narrow widths and was discussed in Ref. 10 as one of the possible candidates for baryonia.

$B(\bar{p}p \to \pi^0 M)$ was obtained from the peak area A (in number of events) above the background according to

$$N_{\bar{p}} B(\bar{p}p \to \pi^0 M) \epsilon_M(2\gamma) B(M \to N_{\rm ch}) = A \ , \qquad (5)$$

where $N_{\bar{p}}$ is the number of stopped antiprotons, $\epsilon_M(2\gamma)$ the effective detection efficiency for $\pi^0 \to 2\gamma$, and $B(M \to N_{\rm ch})$ the decay branching ratio of M into $N_{\rm ch}$-pronged states. $\epsilon_M(2\gamma)$ (see Table II) was calculated by a Monte Carlo procedure within a systematic error of $\pm 5\%$ by simply assuming an invariant phase-space distribution for the decay products of M. The inclusion of the orbital angular momentum between π^0 and M may slightly change the result. This effect may be less important in multiparticle decays of M, since the angular distribution of decay products approaches uniform. In $\bar{p}p \to \pi^0\rho^0$, a typical example of a few-body decays, the dominance of S-state annihilation[3] means that the decay of $\rho^0 \to \pi^+\pi^-$ occurs predominantly in a plane perpendicular to the ρ^0 vector in the rest frame of ρ^0. This effect should reduce the overlap between $\pi^\pm$ and π^0 and give $\epsilon_M(2\gamma)$ somewhere between the two extreme cases of isolated π^0 (no overlap) and π^0 from $\bar{p}p \to \pi^0\rho^0$ with the phase-space distribution (overestimated overlap). From the difference between these two cases, the above effect on $\epsilon_M(2\gamma)$ was estimated to be less than 7% of $\epsilon_M(2\gamma)$. $B(M \to N_{\rm ch})$ (see Table II) was corrected for $\gamma \to e^+e^-$ conversion (6%) in the target as well as in the vacuum chamber walls and for the acceptance (93%) for charged particles.

$N_{\bar{p}}$ is related to N_γ and N_π by

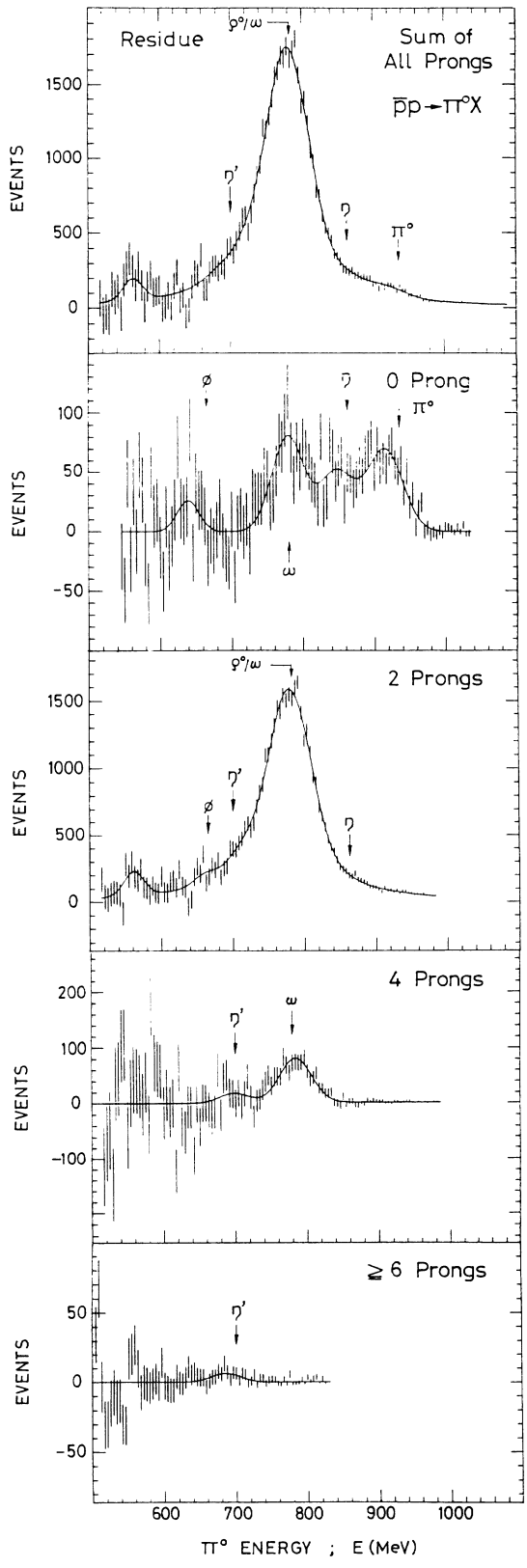

FIG. 7. A fit to the inclusive π^0 spectra is shown in the energy region above 520 MeV after subtracting the polynomial background. Arrows show the expected positions for $\bar{p}p \to \pi^0 M$ for various narrow mesons M.

TABLE I. Results for narrow peaks in the inclusive π^0 spectra. The peak position, peak area, statistical significance, and width (1σ) are given. Except for the $\pi^0\rho^0$ peak, the peaks were fitted with Gaussians, whose width was bound within the instrumental width $\pm 20\%$. The width error given in parentheses indicates that the width was fitted on its lower limit. For the $\pi^0\rho^0/\omega$ peak, see the footnote. To reduce the number of fitting parameters, the widths of some peaks were fixed at the instrumental ones. The averaged peak position is given in Notes.

		Charge multiplicity (N_{ch})				
	N_{ch} = all	0	2	4	6	Notes
Position (MeV)		638.9±5.4	663.2±8.2			646.2±5.4
Events		237±162	611±310			$\bar{p}p \to \pi^0\phi$
Stat. Sig.		1.5σ	2.0σ			
Width (MeV)		18.6(fixed)	15.1(−0, + 5.6)			
Position (MeV)	698.2±25.0		707.1±8.6	698.0±12.0	687.6±7.0	695.9±4.5
Events	277±242		541±320	219±142	51.4±23.2	$\bar{p}p \to \pi^0\eta'$
Stat. Sig.	1.1σ		1.7σ	1.5σ	2.2σ	
Width (MeV)	15.9(fixed)		15.9(−0, + 6.4)	19.7(fixed)	15.6±7.6	
Position (MeV)	771.1±0.6	772.3±14.4	770.4±0.7	783.3±1.9		771.5±0.5
Events	50232±789	1137±181	45175±896	1074±125		$\bar{p}p \to \pi^0\rho^0/\omega$
Stat. Sig.	63.7σ	6.3σ	50.4σ	8.6σ		
Width (MeV)	a	21.3(fixed)	a	21.3(fixed)		
Position (MeV)	872.7±7.9	846.0±4.9	865.5±9.8			855.3±3.8
Events	666±204	715±223	267±169			$\bar{p}p \to \pi^0\eta$
Stat. Sig.	3.3σ	3.2σ	1.6σ			
Width (MeV)	22.9(fixed)	22.6(fixed)	23.0(fixed)			
Position (MeV)	921.8±4.1	913.8±2.6				916.2±2.2
Events	924±140	1064±142				$\bar{p}p \to \pi^0\pi^0/\gamma$
Stat. Sig.	6.6σ	7.5σ				
Width (MeV)	24.1(fixed)	24.0(fixed)				

[a]A Gaussian shape with the instrumental width was assumed for the $\pi^0\omega$ peak with a fixed yield of 4.1×10^{-3} (7240 events for $N_{ch}=2$ and 7930 events for the sum over N_{ch}). The $\pi^0\rho^0$ peak had a Breit-Wigner shape folded in the instrumental resolution.

TABLE II. Detection efficiency $\epsilon_M(2\gamma)$ for $\pi^0\to 2\gamma$ (separated) and $\epsilon_M(1\gamma)$ for $\pi^0\to 2\gamma$ (unseparated) from $\bar{p}p\to\pi^0 M$ for M decaying into N_{ch}-pronged states. B gives the topological decay branching ratios $B(M\to N_{ch})$; both quantities before and after the correction for $\gamma\to e^+e^-$ conversion and for the acceptance for charged particles are given (see the text). $\alpha(2\gamma)$ and $\alpha(1\gamma)$ give the geometrical acceptances (see the text).

Reaction $\bar{p}p\to\pi^0 M$	π^0 Energy (MeV)	$\alpha(2\gamma)$ (isolated π^0)	$\alpha(1\gamma)$	N_{ch}	(B) (uncorr.)	B corr.	$\epsilon_M(2\gamma)$	$\epsilon_M(1\gamma)$
$\bar{p}p\to\ \pi^0\phi$	665.9	0.115	0.0125	0[a]	(11.9%)	10.2%	0.0638	0.0085
				2[a]	(88.1%)	88.1%	0.0789	0.0106
$\pi^0\eta'$	700.0	0.114	0.0161	0	(17.7%)	12.7%	0.0549	0.0098
				2	(69.7%)	64.0%	0.0620	0.0112
				4	(12.6%)	21.9%	0.0645	0.0117
				6	(−)	1.5%	0.0645[b]	0.0117[b]
$\pi^0\omega$	780.0	0.112	0.0249	0	(8.7%)	7.6%	0.0740	0.0215
				2	(91.3%)	82.0%	0.0729	0.0212
				4	(−)	10.4%	0.0729[b]	0.0212[b]
$\pi^0\rho^0$	785.0	0.111	0.0249	2	(100%)	99.5%	0.0780	0.0237
$\pi^0\eta$	862.9	0.109	0.0356	0	(70.9%)	56.4%	0.0738	0.0313
				2	(29.1%)	40.4%	0.0718	0.0322
				4	(−)	3.2%	0.0718[b]	0.0322[b]
$\pi^0\pi^0$	938.3	0.103[c]	0.0903[c]	0	(100%)	88.4%	0.1544[c]	0.0903[c]
$\pi^0\gamma$	943.1	0.101	0.2663[d]	0	(100%)	94.0%	0.0761	0.2463[d]

[a]Effective branching ratio for the present experiment, where decay of $K^\pm$ and K_L was ignored.
[b]The detection efficiencies for four- (six-) prong decays were simply approximated to be the same as for two- (four-) prong ones since the decay topologies were similar.
[c]The detection efficiency listed is already doubled since each of the two π^0's may be detected.
[d]$\alpha(1\gamma)$ and $\epsilon_M(1\gamma)$ listed include the contribution of detection of prompt γ rays (0.220 and 0.20, respectively).

$$N_{\bar{p}} \kappa \int \rho(E')\eta(E')dE' = N_\gamma \tag{6a}$$

and

$$N_{\bar{p}} \int \rho'(E')\epsilon(E')dE' = N_\pi \ , \tag{6b}$$

where $\rho\, dE'$ ($\rho' dE'$) is the number of γ rays (π^0's) with energies between E' and $E'+dE'$ per annihilation and η (ϵ) is the detection efficiency of γ rays (π^0's). κ is a correction factor (1.08) for contamination of fake γ rays, such as unseparated two γ rays from π^0, a single γ ray mistaken as two γ rays, etc. When ρ (ρ') and η (ϵ) were calculated by a Monte Carlo procedure,[12] both relations in Eq. (6) gave the same number, $N_{\bar{p}} = 2.96 \times 10^7$, within $\pm 3\%$.

$B(\bar{p}p \to \pi^0 M)$ was first evaluated separately according to Eq. (5) for each charge multiplicity, and the result is given in Table III. The yields obtained from different $N_{\rm ch}$'s were consistent with each other. They were statistically averaged to give the final yields as

$$B(\bar{p}p \to \pi^0\phi) = (3.0 \pm 1.5) \times 10^{-4} \ , \tag{7a}$$

$$B(\bar{p}p \to \pi^0\eta') = (5.0 \pm 1.9) \times 10^{-4} \ , \tag{7b}$$

$$B(\bar{p}p \to \pi^0\omega) = (5.2 \pm 0.5) \times 10^{-3} \ , \tag{7c}$$

$$B(\bar{p}p \to \pi^0\rho^0) = (1.6 \pm 0.1) \times 10^{-2} \ , \tag{7d}$$

$$B(\bar{p}p \to \pi^0\rho^0/\omega) = (2.1 \pm 0.1) \times 10^{-2} \ , \tag{7e}$$

$$B(\bar{p}p \to \pi^0\eta) = (4.6 \pm 1.3) \times 10^{-4} \ , \tag{7f}$$

$$B(\bar{p}p \to \pi^0\pi^0) = (2.5 \pm 0.3) \times 10^{-4} \ . \tag{7g}$$

Some remarks regarding the derivation of the yield are given below.

For $\bar{p}p \to \pi^0\phi$, besides the dominant two-prong decay of ϕ ($\to K^+K^-$, $\pi^0\pi^+\pi^-$, etc.), the zero-prong decay is also expected from $\phi \to K_L K_S$ with K_L missing and K_S going to $\pi^0\pi^0$. The yield $[(3.0 \pm 1.5) \times 10^{-4}]$ resulted from the two-prong (π^0 energy) spectrum. The result changes little, even if a small peak in the zero-prong spectrum, located about 30 MeV below the expected position, should be included. For $\bar{p}p \to \pi^0\eta'$, the yield $[(5.0 \pm 1.9) \times 10^{-4}]$ came mainly from the two-prong spectrum, while monoenergetic peaks were also observed in the four- and $\geq$ six-prong spectra.

For $\bar{p}p \to \pi^0\omega$, a yield of $(5.2 \pm 0.5) \times 10^{-3}$ was deduced from monoenergetic peaks observed both in the zero-

TABLE III. $B(\bar{p}p \to \pi^0 M)$ (or its upper limit at 95% C.L.) in 10^{-3} deduced from the inclusive π^0 and γ-ray spectra. Each column for specific $N_{\rm ch}$ gives $B(\bar{p}p \to \pi^0 M)$ deduced from the monochromatic peak (or its absence) seen in the $N_{\rm ch}$-prong spectrum. The last column gives the average over different $N_{\rm ch}$'s.

Channel	$N_{\rm ch}=0$	2	4	6	Average over $N_{\rm ch}$
From π^0 spectra					
$\bar{p}p \to \pi^0\phi$		0.30±0.15			0.30±0.15[a]
$\bar{p}p \to \pi^0\eta'$	<1.1	0.46±0.27	0.52±0.34	1.8±0.8	0.50±0.19
$\bar{p}p \to \pi^0\omega$	6.8±1.1	b	4.8±0.6		5.2±0.5
$\bar{p}p \to \pi^0\rho^{0c}$		16±1[b]			16±1
$\bar{p}p \to \pi^0\rho^0/\omega^c$		21±1[b]			21±1
$\bar{p}p \to \pi^0\eta$	0.58±0.18	0.31±0.20			0.46±0.13
$\bar{p}p \to \pi^0\pi^0$	0.25±0.03				0.25±0.03[d]
From γ-ray spectra					
$\bar{p}p \to \pi^0\phi$		<2.4			<2.4[e]
$\bar{p}p \to \pi^0\eta'$	<7.8	<2.9	<3.1		<2.9
$\bar{p}p \to \pi^0\omega$	10±5	b	4.3±2.4		5.4±2.2
$\bar{p}p \to \pi^0\rho^{0c}$		16±4[b]			16±4
$\bar{p}p \to \pi^0\rho^0/\omega^c$		21±3[b]			21±3
$\bar{p}p \to \pi^0\eta$	0.66±0.29	<0.46			0.33±0.21[f]
$\bar{p}p \to \pi^0\pi^0$	0.20±0.07				0.20±0.07[d]

[a]A 1.5σ structure, located about 30 MeV below the expected position in the zero-prong spectrum was not included. Even if this structure is included, the result [Eq. (3a) in Ref. 10] hardly changes.

[b]The $\bar{p}p \to \pi^0\rho^0/\omega$ peak in the two-prong spectrum was fitted with a sum of $\pi^0\rho^0$ and $\pi^0\omega$ peaks by fixing the $B(\bar{p}p \to \pi^0\omega)$ deduced from zero- and four-prong spectra (see the text).

[c]A small interference between $\bar{p}p \to \pi^0\rho^0$ and $\bar{p}p \to \pi^\pm\rho^\mp$ is included (see the text).

[d]$B(\bar{p}p \to \gamma\pi^0) = (1.74 \pm 0.22) \times 10^{-5}$ (Ref. 3) was assumed, though the result hardly depended on the specific value as long as it is much smaller than $B(\bar{p}p \to \pi^0\pi^0)$.

[e]A structure of 2.2σ level, located about 30 MeV below the expected position in the zero-prong spectrum, was not included. Even if this structure is included, the result hardly changes.

[f]We did not include a structure of 3σ level appearing in the four-prong spectrum, since it was located about 30 MeV above the expected position. The systematic error may also be large since the structure is located at the foot of the spectrum close to the base line. Even if this structure is included, the result hardly changes.

prong spectrum corresponding to $\omega \to \pi^0\gamma$ and in the four-prong spectrum corresponding to $\omega \to \pi^+\pi^-\pi^0$ with $\gamma \to e^+e^-$ conversion. The prominent peak at the corresponding energy in the two-prong spectrum may have resulted from contributions due to both $\pi^0\omega$ with $\omega \to \pi^+\pi^-\pi^0$ and $\pi^0\rho^0$ with $\rho^0 \to \pi^+\pi^-$. We tried to separate both channels by using the shape difference of the peaks: the $\pi^0\omega$ peak should be of a sharp Gaussian type with a width close to the instrumental width, while the $\pi^0\rho^0$ peak must be of a broad Breit-Wigner type ($\Gamma = \Gamma_\rho M_\rho / 2M_N = 62.8$ MeV, here M_ρ and M_N being ρ and nucleon rest masses, respectively) folded in the resolution. When the yield of $\pi^0\omega$ exceeded 8×10^{-3}, the fit of the $\pi^0\rho^0/\omega$ peak with a sum of $\pi^0\rho^0$ and $\pi^0\omega$ became poor. This upper limit for $\pi^0\omega$ is compatible with the yield of $\pi^0\omega$ mentioned above. Since we could not distinguish between $\pi^0\omega$ and $\pi^0\rho^0$ precisely enough from the two-prong spectrum, we fixed the yield of $\pi^0\omega$ at the value mentioned above, and determined the yield of $\pi^0\rho^0 = (1.6\pm0.1)\times10^{-2}$, where the quoted error covered the ambiguity in the yield of $\pi^0\omega$. Following a similar procedure we obtained a yield of $(2.1\pm0.1)\times10^{-2}$ for the sum of $\pi^0\omega$ and $\pi^0\rho^0$.

For $\bar{p}p \to \pi^0\eta$, monoenergetic peaks seen in the zero- and two-prong spectra yielded $(4.6\pm1.3)\times10^{-4}$. It should be noted that the phase-space distribution of π^0 in $\bar{p}p \to 3\pi$ (the yield being roughly a few % per annihilation[18]) should be peaked around 850 MeV, which is close to the present peak. The present peak, however, cannot be attributed to the phase-space peak, since the latter should be much broader. For $\bar{p}p \to \pi^0\pi^0$, separation of the $\bar{p}p \to \gamma\pi^0$ peak (at the pion energy of 943 MeV) from the $\bar{p}p \to \pi^0\pi^0$ peak (938 MeV) was difficult. Using a yield of $\gamma\pi^0 = (1.74\pm0.22)\times10^{-5}$ from Ref. 3, we obtained a yield of $\pi^0\pi^0 = (2.5\pm0.3)\times10^{-4}$. This result hardly depends on the value of $B(\bar{p}p \to \gamma\pi^0)$ as long as it is much smaller than 10^{-4}.

V. RESULT ON $\bar{p}p \to \pi^0 M$ AND $\bar{p}p \to \gamma M$ FROM γ-RAY SPECTRA

$\bar{p}p \to \pi^0 M$ with π^0 mistaken as a single γ ray should show up as monoenergetic peaks in the inclusive γ-ray spectra. Such peaks were searched for by fitting the inclusive γ-ray spectra with a polynomial background plus narrow peaks. To reduce the number of adjustable parameters, and to check the stability of the fit, we divided the relevant energy region into two by maintaining an ample overlap between them. Except for $M = \rho^0$, which should have a Breit-Wigner shape, the narrow peaks were expressed by (slightly asymmetric) Gaussian shapes, with the left-right asymmetry determined[12] by an electron beam test.

The fitted result is presented in Figs. 8(a)–8(c) and is also summarized in Table IV for monoenergetic peaks with a statistical significance as high as or higher than 2σ. A large peak (an 8σ effect) was observed at 780 MeV, corresponding to $\bar{p}p \to \pi^0 M$ with $M = \rho^0/\omega$. A few more peaks were observed at 2 to 3σ levels at energies

TABLE IV. Results for narrow peaks in the inclusive γ-ray spectra. The peak position, peak area, statistical significance, and width (1σ) are given. Except for the $\pi^0\rho^0$ peak, the peaks were fitted with Gaussians, whose width was bound within the instrumental width ±20%. The width error given in parentheses indicates that the width was fitted on its upper or lower limit. For the $\pi^0\rho^0/\omega$ peak see footnote. The averaged peak position is given in Notes. No monochromatic peaks were seen in the ≥six-prong spectrum.

		Charge multiplicity (N_{ch})			
	N_{ch} = all	0	2	4	Notes
Position (MeV)		633.6±5.0			633.6±5.0
Events		774±350			$\bar{p}p \to \pi^0\phi$
Stat. Sig.		2.2σ			
Width (MeV)		19.9±6.2			
Position (MeV)	774.4±4.1	772.3±14.4	775.4±3.4	773.2±9.6	774.8±2.5
Events	13773±1802	523±251	11433±1340	291±165	$\bar{p}p \to \pi^0\rho^0/\omega$
Stat. Sig.	7.6σ	2.1σ	8.5σ	1.8σ	
Width (MeV)	a	25.4±5.9	a	25.3(−8.2, + 0)	
Position (MeV)		876.1±8.8		890.4±3.0	880.1±7.2
Events		357±158		122±41	$\bar{p}p \to \pi^0\eta$
Stat. Sig.		2.3σ		3.0σ	
Width (MeV)		18.7(−0, + 7.2)		18.8(−0, + 5.8)	
Position (MeV)	925.6±6.2	923.7±5.9			925.1±6.1
Events	1257±752	613±204			$\bar{p}p \to \pi^0\pi^0/\gamma$
Stat. Sig.	1.7σ	3.0σ			
Width (MeV)	29.1±8.8	19.4(−0, + 9.5)			

[a]A Gaussian shape with the instrumental width was assumed for the $\pi^0\omega$ peak with a fixed yield of 4.7×10^{-3} (2510 events for $N_{ch}=2$ and 2750 events for the sum over N_{ch}). The $\pi^0\rho^0$ peak had a Breit-Wigner shape folded in the instrumental resolution.

corresponding to $M=\eta$, π^0, etc.

Monoenergetic peaks in the inclusive γ-ray spectra may originate not only from two unseparated γ rays from a π^0 produced in $\bar{p}p \to \pi^0 M$ but also from prompt γ rays produced in $\bar{p}p \to \gamma M$. The π^0 energy in $\bar{p}p \to \pi^0 M$ and the γ energy in $\bar{p}p \to \gamma M$ are close to each other, within the instrumental resolution. Since $\bar{p}p \to \gamma M$ is expected to be much less than $\bar{p}p \to \pi^0 M$, due to the smallness of the electromagnetic coupling, below we will first give the yield of $\bar{p}p \to \pi^0 M$ by neglecting $\bar{p}p \to \gamma M$, and then translate it to the upper limit for $\bar{p}p \to \gamma M$.

A. $\bar{p}p \to \pi^0 M$

The yield of $\bar{p}p \to \pi^0 M$ was deduced from the peak area A in the γ-ray spectra according to the following formula:

$$N_{\bar{p}} B(\bar{p}p \to \pi^0 M) \epsilon_M(1\gamma) B(M \to N_{\text{ch}}) = A \ , \tag{8}$$

where $\epsilon_M(1\gamma)$ is the effective detection efficiency for π^0 as a single γ ray. $\epsilon_M(1\gamma)$ was calculated in a similar manner as for $\epsilon_M(2\gamma)$, except for the $\gamma\gamma$ invariant mass cut, and is given in Table II. $N_{\bar{p}}$ was estimated to be 3.08×10^7 according to Eq. (6). $B(\bar{p}p \to \pi^0 M)$ was deduced from the inclusive γ-ray spectrum with each charge multiplicity in a similar way as described in the previous section for the π^0 spectrum, and is given in Table III. The result averaged over the charge multiplicity is also given there in comparison with the result obtained from the inclusive π^0 spectra. Both results are consistent with each other, while the result [Eq. (7)] from the π^0 spectra is of better statistical accuracy. A few remarks regarding the derivation of the result from the γ

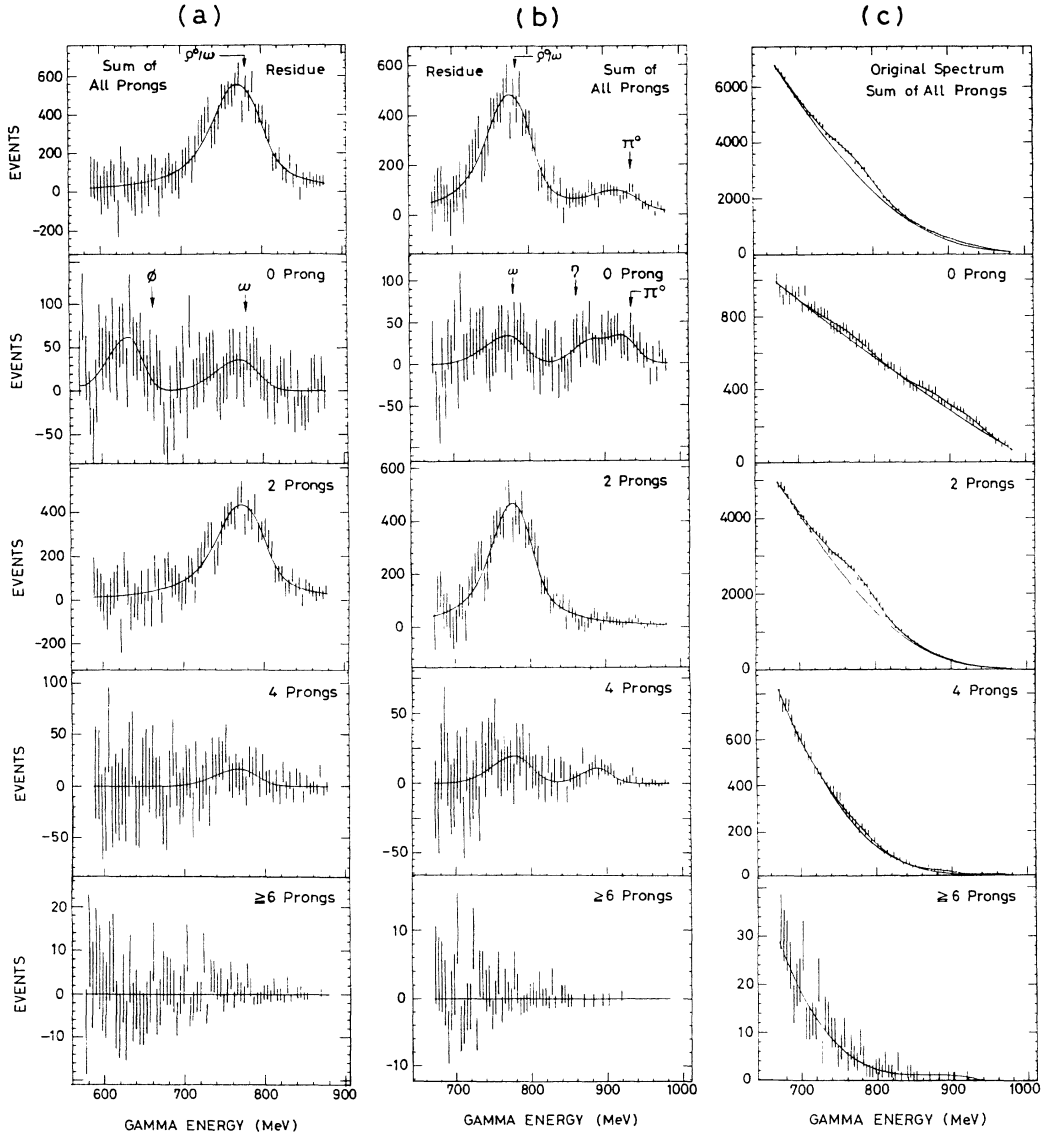

FIG. 8. A fit to the inclusive γ-ray spectra above 590 MeV with a polynomial background plus narrow peaks (see the text). (a) The residue after the background subtraction between 590 and 880 MeV. (b) and (c) The residue and the original spectrum, respectively, between 670 and 980 MeV. Monochromatic peaks obtained with statistical significance higher than or as high as 2σ are included in the fit (solid curves) and also given in Table IV. Arrows indicate the expected positions for $\bar{p}p \to \pi^0 M$ for various narrow mesons M.

spectra are given below.

Similarly to the case of inclusive π^0 spectra, $B(\bar{p}p \to \pi^0\omega) = (5.4 \pm 2.2) \times 10^{-3}$ was deduced from monoenergetic peaks in the zero- and four-prong spectra. The fit of the $\pi^0\omega$ plus $\pi^0\rho^0$ peak in the two-prong spectrum became poor when the yield of $\pi^0\omega$ exceeded 8×10^{-3}. This upper limit is compatible with the $B(\bar{p}p \to \pi^0\omega)$ obtained from the zero- and four-prong spectra. Fixing the $B(\bar{p}p \to \pi^0\omega)$ at the above-mentioned value, we determined the yield of $\pi^0\rho^0$ to be $(1.6 \pm 0.4) \times 10^{-2}$ and the summed yield of $\pi^0\rho^0$ and $\pi^0\omega$ to be $(2.1 \pm 0.3) \times 10^{-2}$. The latter quantity should be equal to that obtained from the inclusive π^0 spectra as the result of the normalization of $\epsilon(1\gamma)$ for this reaction (see Sec. II).

For $\bar{p}p \to \pi^0\pi^0/\gamma$, we determined $B(\bar{p}p \to \pi^0\pi^0) = (2.0 \pm 0.7) \times 10^{-4}$ using the existing result[3] of $B(\bar{p}p \to \pi^0\gamma) = (1.74 \pm 0.22) \times 10^{-5}$.

B. $\bar{p}p \to \gamma M$

The upper limits for $B(\bar{p}p \to \gamma M)$ were obtained by attributing the monoenergetic peaks observed in the γ-ray spectra entirely to $\bar{p}p \to \gamma M$. They were calculated according to Eq. (8) with $\epsilon_M(1\gamma)$ replaced by η_M, the detection efficiency for γ rays. We used a simplified formula:

$$B(\bar{p}p \to \gamma M) < B(\bar{p}p \to \pi^0 M) \langle \epsilon_M(1\gamma) \rangle / \langle \eta_M \rangle \ , \quad (9)$$

where $\langle\ \rangle$ stands for the average over the decay modes of M. This is justified because neither $\epsilon_M(1\gamma)$ nor η_M depends much on $N_{\rm ch}$; the smallness of the dependence of $\epsilon_M(1\gamma)$ on $N_{\rm ch}$ is demonstrated in Table II, and that of η_M in Fig. 23 of the second paper of Ref. 12. $\langle \epsilon_M(1\gamma) \rangle$ was obtained by averaging the $\epsilon_M(1\gamma)$ given in Table II. $\langle \eta_M \rangle$, calculated by a Monte Carlo procedure, was 0.16 for $M = \eta'$, 0.19 for ϕ and ω, and 0.20 for ρ^0, η, and π^0. We obtained the following results:

$$B(\bar{p}p \to \gamma\phi) < 1.4 \times 10^{-4} \ \ (95\%\ \text{C.L.}) \ , \quad (10a)$$

$$B(\bar{p}p \to \gamma\eta') < 2.0 \times 10^{-4} \ \ (95\%\ \text{C.L.}) \ , \quad (10b)$$

$$B(\bar{p}p \to \gamma\omega) < 9.6 \times 10^{-4} \ \ (95\%\ \text{C.L.}) \ , \quad (10c)$$

$$B(\bar{p}p \to \gamma\rho^0/\omega) < 2.9 \times 10^{-3} \ \ (95\%\ \text{C.L.}) \ , \quad (10d)$$

$$B(\bar{p}p \to \gamma\eta) < 8.7 \times 10^{-5} \ \ (95\%\ \text{C.L.}) \ , \quad (10e)$$

$$B(\bar{p}p \to \gamma\pi^0) < 5.3 \times 10^{-5} \ \ (95\%\ \text{C.L.}) \ . \quad (10f)$$

The upper limit of Eq. (10f), which was several times more stringent than that given by Eq. (9), was obtained from a comparison between the inclusive π^0 and γ-ray spectra in the following way. Since the two monochromatic π^0 or γ-ray peaks of $\bar{p}p \to \pi^0\pi^0$ and $\bar{p}p \to \gamma\pi^0$ overlapped each other, there was an ambiguity regarding the division into two channels. If $\gamma\pi^0$ was assumed to overwhelm $\pi^0\pi^0$, the yield of $\gamma\pi^0$ should be $(5.3 \pm 0.7) \times 10^{-4}$ from the inclusive π^0 spectra and $(9.1 \pm 3.1) \times 10^{-5}$ from the inclusive γ-ray spectra; these two values are inconsistent with each other. Equation (10f) was then determined so that the above two values should become consistent with each other within the (sum of) 2σ errors. We neglected $\bar{p}p \to \gamma\gamma$, as it should be much less abundant than $\gamma\pi^0$ (Refs. 3 and 11).

VI. SUMMARY AND DISCUSSION

Using modularized NaI detectors we carried out highly statistical measurements of the inclusive π^0 and γ-ray spectra, separately for each charge multiplicity of the final state. We derived the yield of $\bar{p}p$ annihilation into $\pi^0 M$ for $M = \phi$, η', ω, ρ^0, η, and π^0 from both the inclusive π^0 and inclusive γ-ray spectra. The systematic error was within 15% for the result derived from the π^0 spectra (except for $M = \phi$ which is described later) and 20% for the result from the γ-ray spectra; it came mainly from the fitting condition of the spectra and from the Monte Carlo of the detection efficiencies. The result from the π^0 spectra is of statistically much higher accuracy than that from the γ-ray spectra, and is given in Eq. (7); both results are consistent with each other as seen in Table III.

$B(\bar{p}p \to \pi^0\rho^0)$ of Eq. (7d) corresponds to $|A(\pi^0\rho^0)|^2 + X$, where $A(\pi^0\rho^0)$ denotes the transition amplitude $\langle \pi^0\rho^0 | H | \bar{p}p \rangle$ and X the interference term of $2\,\text{Re}\{A(\pi^0\rho^0)[A^+(\pi^-\rho^+) + A^+(\pi^+\rho^-)]\}$. X was estimated to be less than 10% of $|A(\pi^0\rho^0)|^2$ from the Dalitz plot[19] of $\bar{p}p \to \pi^0\pi^+\pi^-$ by comparing the number of events lying in the ρ^0 band and in the region where the ρ^0 and $\rho^\pm$ bands cross. Even if the above ambiguity in X is considered, Eq. (7d) is consistent with the bubble-chamber result of $(1.4 \pm 0.2) \times 10^{-2}$ (Ref. 19) which should correspond to $|A(\pi^0\rho^0)|^2$.

We obtained $B(\bar{p}p \to \pi^0\pi^0)$, Eq. (7g), by assuming $B(\bar{p}p \to \gamma\pi^0) = (1.74 \pm 0.22) \times 10^{-5}$ (Ref. 3). It is roughly consistent with the previous experimental results: $(2.06 \pm 0.14) \times 10^{-4}$ from Ref. 3, $(1.4 \pm 0.3) \times 10^{-4}$ from Ref. 2, and $(4.8 \pm 1.0) \times 10^{-4}$ from Ref. 1. Substituting it and $B(\bar{p}p \to \pi^+\pi^-)$ of $(3.2 \pm 0.3) \times 10^{-3}$ (Ref. 19) into Eq. (1), we obtain an R of $(23 \pm 4)\%$ which is in agreement with $(18 \pm 2)\%$ of Ref. 3.

The obtained yields of $\pi^0\omega$, $\pi^0\eta'$, and $\pi^0\eta$ are considerably smaller than the previous experimental values from,[20] which were obtained indirectly by a shape analysis of the inclusive γ-ray spectrum. Regarding $\bar{p}p \to \pi^0\eta'$ and $\pi^0\eta$, the QLR approach[6] predicts $\bar{\sigma}(\pi^0\eta') = K\bar{\sigma}(\pi^0\eta)$, where $\bar{\sigma}(ab)$ is the reduced cross section $\sigma(\bar{p}p \to ab)/q^{2L+1}$ with q and L the momentum and the orbital angular momentum in the final state, respectively, and K is a constant depending on the mixing angle $\theta_{\rm PS}$. L is allowed to be 0 or 2. K becomes approximately 1.0 (0.38) when $\theta_{\rm PS}$ is $-10°$ ($-23°$) (Ref. 21) from the quadratic (linear) version of the mass formula. The present result on $B(\bar{p}p \to \pi^0\eta')$ and $B(\bar{p}p \to \pi^0\eta)$ is consistent with two sets of ($L = 0$, $\theta_{\rm PS} = -10°$) and ($L = 2$, $\theta_{\rm PS} = -23°$). Consequently, a future measurement of L would be interesting because it could show that $\theta_{\rm PS} = -10°$ or $-23°$. Both $B(\bar{p}p \to \pi^0\eta')$ and $B(\bar{p}p \to \pi^0\eta)$ are much smaller than $B(\bar{p}p \to \pi^0\omega)$ in the isovector sector for the final states. This should be compared with the fact that $B(\bar{p}p \to \pi^0\pi^0)$ is much smaller than $B(\bar{p}p \to \pi^0\rho^0)$ in the isoscalar sector. These relations may be interpreted in terms of the small P-wave annihila-

tion. Equations (7f) and (7g) give $\bar{\sigma}(\pi^0\eta)/\bar{\sigma}(\pi^0\pi^0)$ of approximately unity for $L=0$ and more than unity for $L=2$. This value is too large to be explained in terms of purely rearrangement graphs, and indicates[8] the importance of the annihilation graphs.

$B(\bar{p}p \to \pi^0\phi)$, Eq. (7a), may suffer from a larger systematic error than for the other reactions due to the fact that an additional $\pi^0\delta^0$ peak may be located close to the $\pi^0\phi$ peak with a similar yield level.[22] The position and the decay topology of the observed peak, however, preferred $\pi^0\phi$ to $\pi^0\delta^0$. Equation (7a) is consistent with an experimental data of $B(\bar{p}n \to \pi^-\phi) = (3.5 \pm 0.6) \times 10^{-4}$ (Ref. 23). An order of magnitude smaller yield for $\pi^0\phi$ than for $\pi^0\omega$ is explainable in terms of the Okubo-Zweig-Iizuka rule.[24]

The upper limit for radiative decay $\bar{p}p \to \gamma M$ is given in Eq. (10), for which the systematic error was as large as 20%. There exists no previous experimental data that the present result can be compared with, except for the $\gamma\pi^0$ channel. The upper limit for $B(\bar{p}p \to \gamma\pi^0)$, Eq. (10f), is consistent with a recent experimental value of $(1.74 \pm 0.22) \times 10^{-5}$ (Ref. 3) and is inconsistent with an older one.[20] When $B(\bar{p}p \to \pi^0\omega)$ of Eq. (7c) and $B(\bar{p}p \to \pi^0\rho^0)$ of Eq. (7d) are substituted, Eq. (2) predicts $B(\bar{p}p \to \gamma\pi^0)$ to be 1.2×10^{-4} for $\cos\beta' = 1$, 8.6×10^{-5} for $\cos\beta' = 0$, and 5.4×10^{-5} for $\cos\beta' = -1$. The destructive interference ($\cos\beta' = -1$) is compatible with the present result [Eq. (10f)], while a factor of 3 times larger than the experimental result of Ref. 3 cited above. While $\cos\beta'$ gives the interference between the isoscaler and isovector amplitudes for the initial ^3S state of $\bar{p}p$, a corresponding quantity of $\cos\beta$ (Ref. 11) for the initial ^1S state can be obtained from, for example, $B(\bar{p}p \to \gamma\omega)$. The upper limit for $B(\bar{p}p \to \gamma\omega)$, Eq. (10c), is, however, still a few times as large as the theoretical estimate,[11] with the interference neglected. An improvement in the sensitivity by an order of magnitude is necessary in order to determine $\cos\beta$ from the above reaction.

ACKNOWLEDGMENTS

The authors would like to express their deep thanks to Professor T. Nishikawa, Professor S. Ozaki, Professor H. Sugawara, and Professor H. Hirabayashi for supporting the present work. They are indebted to the staff of the computer center of KEK, especially to Professor S. Kabe, Professor Y. Miura, and Dr. O. Hamada, for help regarding the computation technique. They are indebted to Professor L. Tauscher for helpful discussions concerning various problems in the analysis, to Professor T. Ueda, Professor S. Furui, and Professor M. Maruyama for stimulating discussions in which various theories were compared, and to Professor T. Yukawa for elucidating the interference of different charge states in the measurement of $\bar{p}p \to \pi^0\rho^0$.

*Present address: Kochi Medical School, Nankoku, Kochi 781-51, Japan.

†Present address: National Laboratory for High Energy Physics (KEK), Tsukuba, Ibaraki 305, Japan.

[1]S. Devons *et al.*, Phys. Rev. Lett. **27**, 1614 (1971).

[2]G. Bassompierre *et al.*, in *Proceedings of 4th European Antiproton Symposium*, Barr, 1978, edited by A. Fridman (Editions du CNRS, Paris, 1979), Vol. 1, p. 139.

[3]L. Adiels *et al.*, Z. Phys. C **35**, 15 (1987).

[4]S. Ahmad *et al.*, in *Proceeding of the 3rd LEAR Workshop*, Tignes, 1985, edtied by U. Gastaldi *et al.* (Editions Frontières, Gif-sur-Yvette, France, 1986), p. 353.

[5]T. B. Day, G. A. Snow, and J. Sucher, Phys. Rev. Lett. **3**, 61 (1959); R. Knop *et al.*, *ibid.* **14**, 767 (1965); R. A. Rubinstein *et al.*, *ibid.* **15**, 639 (1965).

[6]H. Genz, Phys. Rev. D **28**, 1094 (1983); **31**, 1136 (1985).

[7]S. Okubo, Prog. Theor. Phys. Suppl. **63**, 1 (1978).

[8]C. B. Dover and P. M. Fishbane, Nucl. Phys. **B244**, 349 (1984).

[9]U. Hartmann, E. Klempt, and J. G. Korner, Phys. Lett. **155B**, 163 (1985).

[10]M. Chiba *et al.*, Phys. Lett. B **202**, 447 (1988).

[11]B. Delcourt, J. Layssac, and E. Palaquier, in *Proceedings of the Workshop on Physics at LEAR with Low Energy Cooled Antiprotons*, Erice, 1982, edited by U. Gastaldi and R. Klapisch (Plenum, New York, 1984), p. 305.

[12]M. Chiba *et al.*, Phys. Lett. B **177**, 217 (1986); Phys. Rev. D **36**, 3321 (1987).

[13]M. Kobayashi *et al.*, Nucl. Instrum. Methods **A245**, 59 (1986).

[14]R. L. Ford and W. R. Nelson, Report No. SLAC-210, 1978 (unpublished).

[15]B. Rossi, *High Energy Particles* (Prentice Hall, New York, 1952).

[16]M. Chiba *et al.* (unpublished).

[17]F. James and M. Roos, Comput. Phys. Commun. **10**, 343 (1975).

[18]R. Armanteros and B. French, in *Antinucleon-Nucleon Interactions in High Energy Physics*, edited by E. H. S. Burhop (Academic, New York, 1969), Vol. IV, p. 237.

[19]C. Baltay *et al.*, Phys. Rev. **145**, 1103 (1966).

[20]G. Backenstoss *et al.*, Nucl. Phys. **B228**, 424 (1983).

[21]Particle Data Group, M. Aguilar-Benitez *et al.*, Phys. Lett. **170B**, 1 (1986).

[22]$\bar{p}p \to \pi^\pm\delta^\mp$ is allowed from the $I=0$, $^1S_0\bar{p}p$ state while $\bar{p}p \to \pi^0\delta^0$ is allowed from the $I=1$, $^3P_1$ one. Although, to the authors' knowledge, existence of $\bar{p}p \to \pi\delta$ has not yet experimentally been established, a preliminary value on $B(\bar{p}p \to \pi^\pm\delta^\mp) = (2.5 \pm 0.4) \times 10^{-3}$ is seen in C. Amsler, *8th European Symposium on $N\bar{N}$ Interactions*, Thessaloniki, 1986, edited by S. Charalambous *et al.* (World Scientific, Singapore, 1986), p. 159. This value together with the amount of P-wave annihilation of about 20% (Ref. 3) predicts a yield of $(2.5 \pm 0.4) \times 10^{-4}$ for $\pi^0\delta^0$.

[23]L. Gray *et al.*, Phys. Rev. D **27**, 307 (1983).

[24]S. Okubo, Phys. Lett. **5**, 165 (1963); G. Zweig, CERN Reports Nos. TH-401 and TH-412, 1964 (unpublished); J. Iizuka, Prog. Theor. Phys. Suppl. **37-38**, 21 (1966).